

Evaporative Heat Transfer with R134a in a Vertical Minichannel

Zahid Anwar¹

1. Mechanical Engineering Department, University of Engineering and Technology Lahore, Pakistan.
zahidanwar@uet.edu.pk

Abstract

Smart cooling solutions are required for modern electronic devices as heat flux is continuously increasing while component size is shrinking day by day. Two phase heat transfer within compact channels can cope with high heat flux applications. Two phase heat transfer in narrow channels was the subject of many studies from last decade. The mechanisms involved, however, are not fully clear and there is still room for further investigations to come up with a general solution. This article reports experimental finding on flow boiling heat transfer of R134a in a resistively heated, smooth vertical stainless steel minichannel. Experiments were conducted at 27 & 32 °C saturation temperature with 100-500 kg/m²s mass flux and till completion of dryout. The effect of various parameters like, heat flux, mass flux, vapor quality and system pressure was studied. Results indicated that heat transfer was strongly controlled by applied heat flux while insignificant effect of varying mass flux and vapor quality was observed. Experimental findings were compared with various macro and micro scale correlations from literature, this comparison revealed Gungor and Winterton [10] correlation as the most accurate one for predicting local heat transfer coefficients.

Key Words: Flow boiling, heat transfer, heat exchanger, heat flux, heat transfer, coefficient

1. Introduction

Boiling becomes the obvious choice for transferring high heating/cooling loads over small temperature lifts. As per Kandlikaar [1], channels with hydraulic diameter within 200µm-3mm range are considered as minichannels. Compactness in size offer many potential benefits like, enhanced heat transfer (increased surface area), less fluid inventory, less material cost etc.

Callizo [2] conducted flow boiling experiments with R134a in a resistively heated 0.64 mm vertical stainless steel channel. Experiments were conducted at 30 and 35 °C saturation temperature and with 185-335 kg/m²s mass fluxes. He found nucleate boiling dominance mechanism, where heat transfer was strongly controlled by applied heat flux and no significant contribution from mass flux and quality was observed.

Owhaib [3] conducted flow boiling heat transfer with R134a in 1.7, 1.224 and 0.826 mm vertical channels and found similar trends as those of Callizo [2].

Ali [9] reported dryout result for R134a in vertical, single stainless steel tubes (1.22 and 1.7 mm

inside diameter and 220 mm heated length) at two operating pressures corresponding to 27 and 32 °C saturation temperatures, other operating parameters were mass flux 50-600 kg/m²s. They noticed that dryout heat flux increased with increasing mass flux, decreased with reducing tube diameter while remains unchanged with varying operating pressure.

Maqbool [8] conducted flow boiling experiments for ammonia in vertical minichannels (1.7 and 1.224 mm inside diameter), tests were conducted at 23, 33 and 43 °C saturation temperature and with mass flux 100-500 kg/m²s. They found nucleate boiling dominance in large channel, whereas smaller channel showed different behavior (at higher qualities heat transfer did increased with increasing vapor fraction)

Tibrica [4] conducted experimental study on flow boiling of R134a and R245fa in a resistively heated horizontal stainless steel tube (2.3 mm inside diameter). Experiments were conducted at three saturation temperatures within 22-41 °C and with 50-700 kg/m²s mass flux. They observed presence of both nucleate and convection boiling mechanisms in their data base.

Ong [5] worked with R134a, R245fa & R236fa as the working fluids and performed experiments using a 1.03 mm stainless steel channel with 200-1600 kg/m²s mass flux and till dryout conditions. They observed nucleate boiling dominance in their data at low quality conditions (Isolated bubble flow) whereas noticeable convective contribution was there for annular flow regime.

Literature review revealed different mechanisms quoted by different research groups, furthermore there is no general agreement for the prediction methods as well. Surface roughness may have significant effects on bubble nucleation process in such small channels, however, this information was missing in many experimental studies in the literature. This experimental study is therefore conducted with R134a in a single vertical channel (till dryout completion) under stable conditions with surface characterization of heating surface. Main objectives are to add reliable set of experimental data into the literature, to trace out dominant mechanisms and to assess the correlations. Details of experimental setup, parametric effects on flow boiling heat transfer and assessment of correlations can be found in following sections.

2. Experimental Setup

Experimental setup consists of a closed loop system schematically shown in Figure 1. Test section was heated by Joule's effect using DC power supply and a water cooled plate type heat exchanger was used to condense the vaporized refrigerant. Stainless steel tube (1.6 mm inside diameter and 245 mm heated length) with upward flow orientation was used as a test section. Eight equally spaced thermocouples were attached on the outer wall to record the wall temperature while insertion type thermocouples were used to record the bulk fluid temperature (at the inlet and outlet of test section). Figure 2 shows graphically the test section before and after fixing thermocouples.

Gear pump was used to circulate the fluid through the loop. System pressure was recorded by an absolute pressure sensor while pressure drop across the test section was measured by a differential pressure sensor. To electrically isolate the test section from other parts, similar sized glass tubes were used before the inlet and after the outlet of the test section.

A 2 μm filter was placed before the inlet of test section to prevent entry of any small particles. Mass flow rate was recorded by a Coriolis mass flow meter. Data logger was connected with computer and HP Agilent VEE was used for data acquisition purpose.

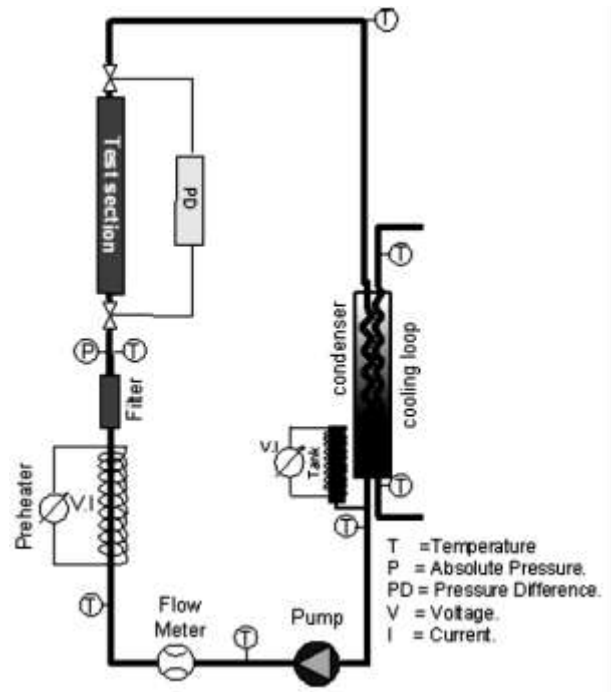


Fig. 1 Schematic diagram of the experimental setup



Fig. 2 Test section before and after attaching thermocouples

Sufficient time was given after adjusting the system pressure and mass flow rate to achieve the steady state conditions, heat flux was then applied in small increments. After dryout incipience heat flux was increased in very small steps (about 1 kW/m²) till the completion of dryout. About 100

data-points were recorded for each applied heat flux and their mean value was then used in the calculation. REFPROP 9 (Reference fluid thermodynamic and transport properties database, developed by NIST) was used to get the refrigerant property data.

Roughness for the inner surface of the test section was checked with stylus methodology, Fig. 3 shows the roughness profile while table 1 summarizes the main parameters for this. Surface roughness has an influence on bubble nucleation which in turn controls the heat transfer process. Surface roughness profile and values are given to help readers for comparative analysis with other studies.

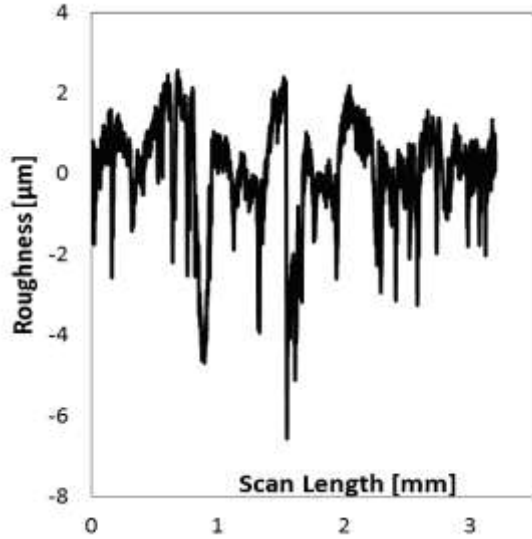


Fig. 3 Roughness profile for the inner surface of the test section

Table 1: Roughness values

Ra ¹ [μm]	Rp ² [μm]	Rv ³ [μm]
0.95	2.69	6.44

3. Data Reduction

Heat flux applied to the test section was calculated by,

$$q'' = \frac{V.I}{A_h} \quad (1)$$

Where I and V are the applied current and voltage respectively. A_h is the heated area, $A_h = \pi d_{in} l$

Inner wall temperature was calculated from the outer wall temperature by using the solution of steady state one dimensional heat conduction equation (with heat generation) for cylinders [3], given by,

$$t_{wall\ in} = t_{wall\ out} + \frac{Q}{4\pi k l} \left[\frac{\xi(1 - \ln \xi) - 1}{\xi - 1} \right] \quad (2)$$

Where $\xi = \frac{d_{out}^2}{d_{in}^2}$ and Q is the applied heat power.

Bulk temperature at any axial location (under subcooled conditions) was calculated with the information of bulk inlet temperature and applied heat by,

$$t_{fluid\ z} = t_{fluid\ in} + \frac{q'' \pi d_{in}}{m C_p} z \quad (3)$$

Local heat transfer coefficient at any location was calculated by,

$$h_z = \frac{q''}{t_{wall\ in} - t_{sat}} \quad (4)$$

Quality/vapor fraction at any axial location is calculated by,

$$x_{th} = \frac{q'' \pi d_{in} (z - z_o)}{A_c G h_{fg}} \quad (5)$$

Where $z - z_o$ is the boiling length and h_{fg} is the latent heat of vaporization.

$$z_o = \frac{m' C_p (t_{sat} - t_{in})}{q'' \pi d_{in}} \quad (6)$$

4. Results and Discussion

Boiling curves for all five mass fluxes at 32 °C saturation temperature are shown in Figure 4. This

¹ Arithmetic mean value for the roughness

² Maximum peak height

³ Maximum valley depth

figure shows variation of heat flux against wall superheat (local wall temperature from the last thermocouple was used). Two distinct regions are clear in this boiling curve, initially there is a sharp increase in heat flux with a slight increase in the wall superheat and this follows with the reverse trend in the end showing the dryout conditions (sharp increase in superheat with a slight increase in applied heat flux).

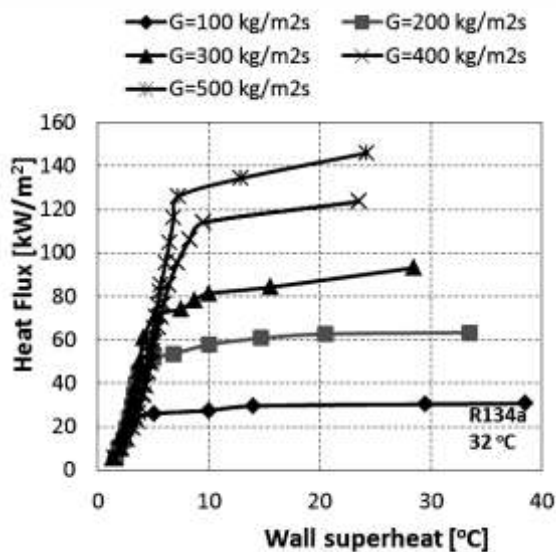


Fig. 4 Boiling curve with 100-500 kg/m²s and at 32 °C saturation temperature

Effect of heat flux is shown in Figure 5, this shows variation of local heat transfer coefficient with vapor quality at different applied heat fluxes for 500 kg/m²s and at saturation temperature of 32 °C. It is clear from the figure the heat transfer coefficients increased with increasing heat flux. For all plots slightly lower heat transfer coefficients were observed with third thermocouple, this could be possibly due to attachment related problem with this thermocouple.

Figure 6 shows the effect of mass flux and vapor quality on local heat transfer coefficient, at a constant heat flux of 50 kW/m² and at saturation temperature of 27 °C. Similar values for heat transfer coefficients with varying mass flux were obtained, furthermore before dryout incipience (for 200 and 300 kg/m²s) no significant effect of vapor quality was there. Similar trends were observed at other operating conditions (heat fluxes and saturation temperature).

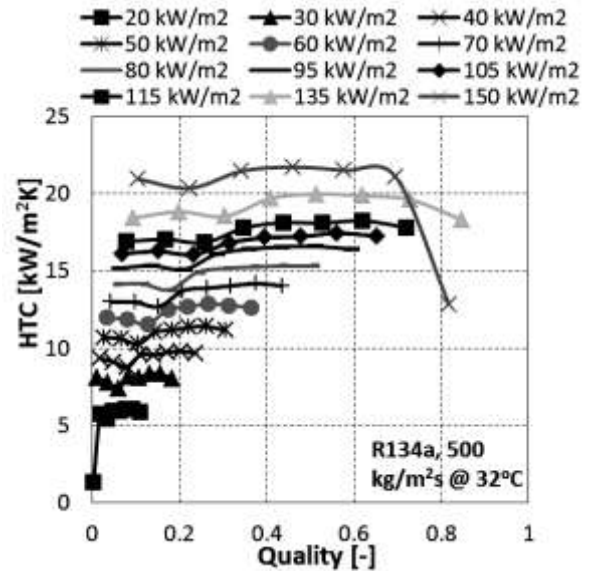


Fig. 5 Effect of heat flux on heat transfer coefficient

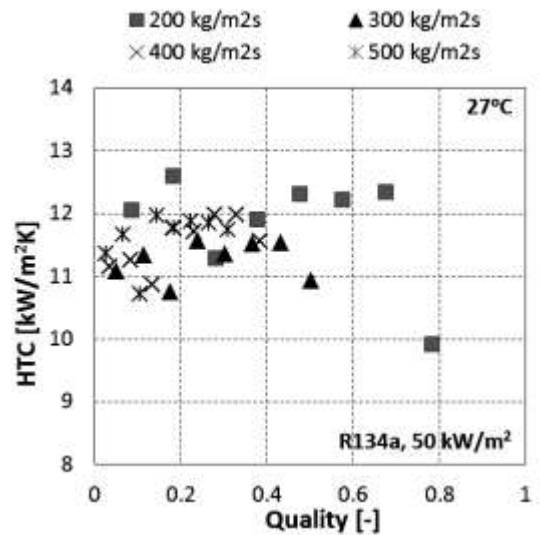


Fig. 6 Variation of heat transfer coefficient with mass flux and vapor quality

Effect of varying system pressure is shown in figure 7 where local heat transfer coefficients at two operating pressures (7.05 and 8.15 bar) are shown against vapor quality. Increase in system pressure did increase in heat transfer as can be observed in Figure 7. Increased system pressure results in reduced vapor velocity and hence lower suppression of nucleate boiling, this could possibly be the reason behind improved heat transfer.

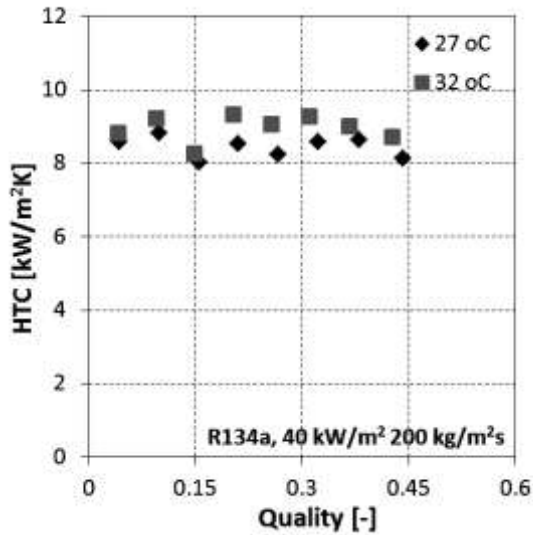


Fig. 7 Effect of system pressure on local heat transfer coefficient

Strong dependency of heat transfer coefficient on applied heat flux is widely explained in the literature by the dominance of nucleate boiling mechanism, however the same could also be explained by thin film evaporation mechanism (bubble nucleation occurs in the close vicinity of the upstream end of the test section and then bubble gets elongated along its flow through the tube, without any additional nucleation, and hence forms a thin liquid layer at the walls, the evaporation of this thin film has resemblance with the nucleate boiling mechanism). Similar parametric effects (insignificant convective contribution) were reported by many authors like, Tran with R12 in 2.46 mm tube [6], Lazarek and Black for R113 [7], Maqbool [8] for ammonia and propane in 1.70 mm vertical tube, Ali [9] with R134a in 1.7 mm tube.

5. Comparison with Correlations

This section describes comparison of experimental data with correlations from literature; data was compared by considering mean bias error [MBE] and % age of data within $\pm 30\%$ from experimental values. MBE gives information about variance of predicted values from experimental ones and is calculated

$$\text{by } MBE = \frac{1}{N} \left(\sum \frac{h_{\text{Predicted}} - h_{\text{Experimental}}}{h_{\text{Experimental}}} \right) * 100$$

Mathematical formulation for the correlations and summary of comparison can be found in table 2.

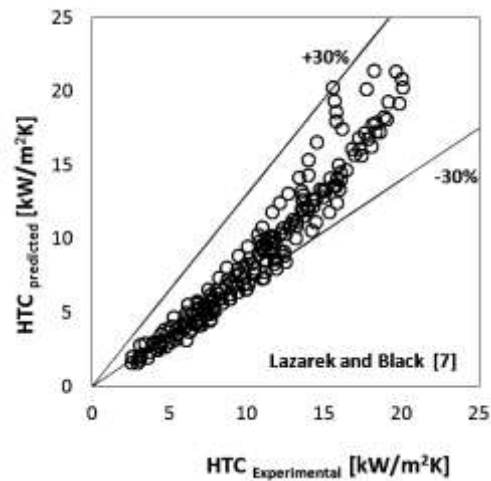
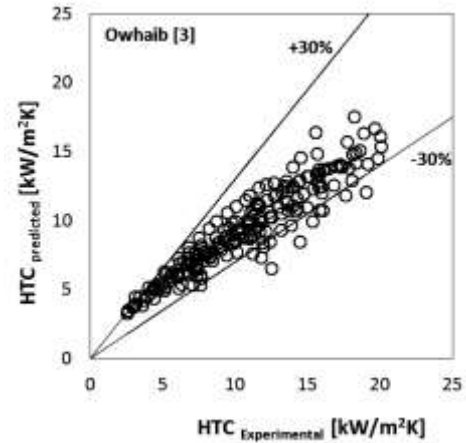
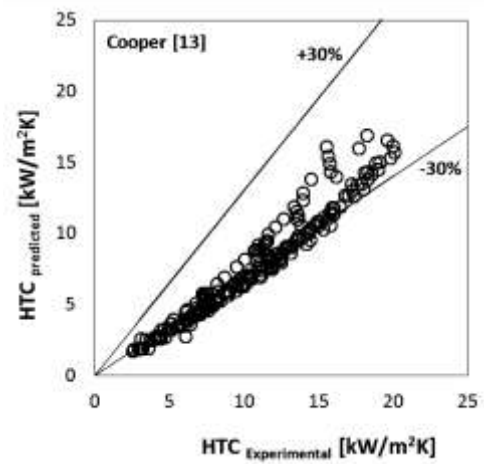


Fig. 8 Comparison with correlations for average heat transfer coefficient

Average heat transfer coefficients were compared with Cooper's pool boiling correlation [13], this correlation was proposed for estimating pool boiling heat transfer however good predictions for flow boiling in minichannels were reported by many authors [2, 8, 9]. Comparison revealed accurate prediction with this correlation however data was mostly underpredicted. Accurate predictions were noticed by changing the leading multiplier to 60 instead of 55 in the original correlation.

Accurate prediction for average heat transfer coefficients were noticed with Lazarek and Black [7] and Owhaib's [3] correlations as can be seen in Figure 8. Both consider strong contributions from nucleate boiling effect (similar trends were observed in this study) which is reflected from the presence of boiling number in these correlations.

Local heat transfer coefficients were also compared with the predictions from several correlations. Predictions with Gungor and Winterton [10], Kew and Cornwell [11] & Bertsch [12] correlations are shown in Figure 9. Accurate predictions were observed with Gungor and Winterton correlation [10] and this was followed by Kew and Cornwell [11] and Bertsch correlations [12].

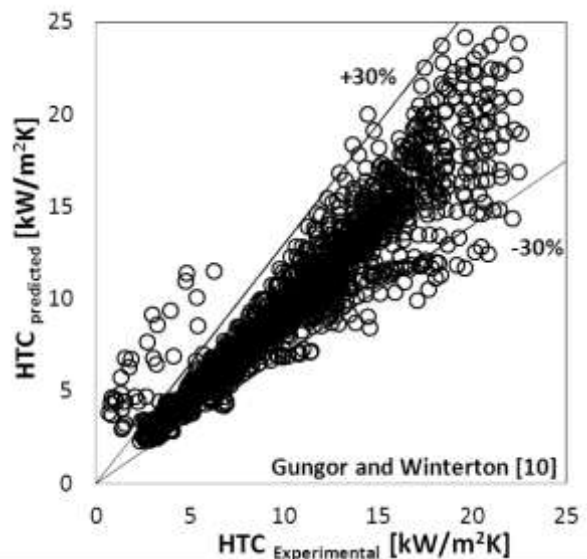
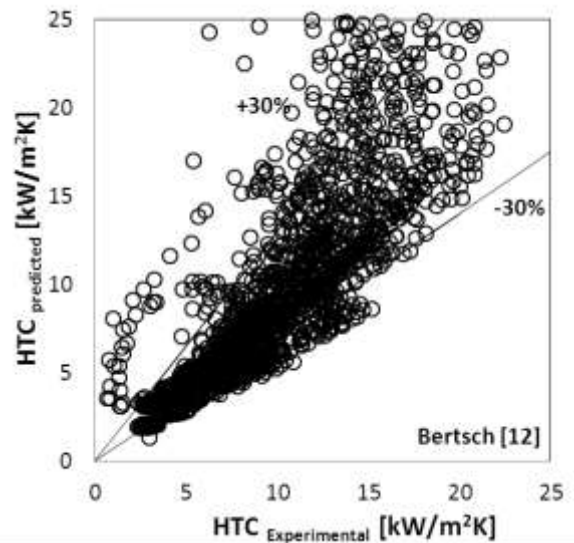
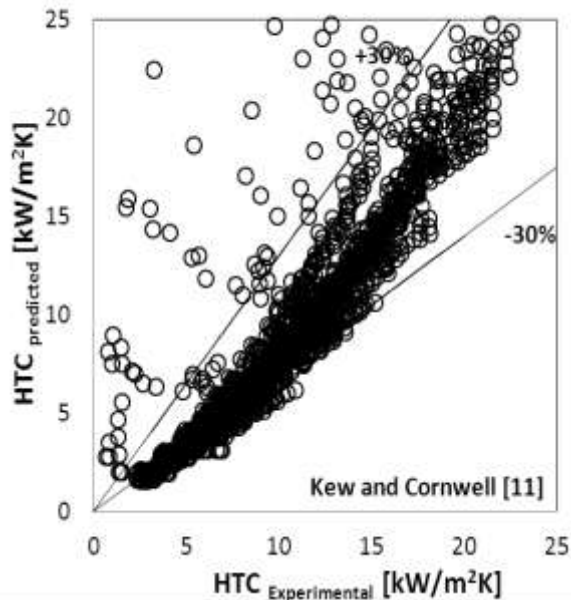


Fig. 9 Comparison of local heat transfer coefficients with correlation from literature

Gungor and Winterton [10] correlation was derived from a large database (involving many fluids) and considers contributions from nucleate and convective boiling mechanisms. As the correlation was developed from a large data base under wide operating conditions, furthermore this considers contributions from both boiling mechanisms (nucleate and convective) with suppression and enhancement factors, this may closely followed the actual evaporation process in this minichannel.

Table 1 Summary of comparison with correlation

Sr. No	Correlation	Expression	MBE	Percentage of data
1	Cooper [13]	$h = 55P_R^{0.12} (-\log_{10} P_R)^{-0.55} M^{-0.5} q^{0.67}$	29.38	44.33
2	Lazarek and Black [7]	$h = 30\text{Re}_{lo}^{0.857} \text{Bo}^{0.714} \frac{K_l}{d_{in}}$	20.98	75.86
3	Kew and Cornwell [11]	$h = h_{\text{Lazarek and Black}} (1-x)^{-0.143}$	10.53	73.27
4	Gungor and Winterton [10]	$h = Eh_{D-B} + Sh_{\text{Cooper}}$ $E = 1 + 2400\text{Bo}^{1.16} + 1.37 \left(\frac{1}{X_{tt}} \right)^{0.86}$ $S = (1 + 1.15 \times 10^{-6} E^2 \text{Re}_l^{1.17})^{-1}$	13.78	95.07
5	Liu and Winterton [14]	$h_{tp}^2 = (Eh_{D-B})^2 + (Sh_{\text{Cooper}})^2$ $E = \left[1 + x \text{Pr} \left\{ \frac{\rho_l}{\rho_g} - 1 \right\} \right]^{-0.35}$ $S = \left[1 + 0.055E^{0.1} \text{Re}_{lo}^{0.16} \right]^{-1}$	39.63	17.67
6	Owhaib [3]	$h_{tp} = 40(\text{Re}_{lo} \text{Bo})^{0.5} (1-x_{\text{exit}})^{0.1} \text{Co}^{0.55} \text{PR}^{1.341} \left(\frac{\rho_l}{\rho_g} \right)^{0.37} \frac{k_l}{d_{in}}$	14.53	92.11
7	Bertsch [12]	$h = Sh_{nb} + Fh_{\text{conv}} \quad h_{nb} = h_{\text{Cooper}}$ $S = (1-x) \quad h_{\text{conv}} = (1-x)h_{Lo} + xh_{go}$ For turbulent flow h_{Lo} and h_{go} are calculated from Dittus boelter equation. For laminar flow $h_{Lo/go} = \frac{k_{l/g}}{D} \left\{ 3.66 + \frac{0.068 \frac{d}{l_h} \text{Re}_{lo/go} \text{Pr}_{l/g}}{1 + 0.04 \left(\frac{d \text{Re}_{lo/go}}{l_h} \right)^{2/3}} \right\}$	32.35	64.47
8	Mikielewicz [15]	$\frac{h_p}{h_{Lo}} = \sqrt{\phi_{MS}^2 + \frac{1}{1+p} \left[\frac{h_{nb}}{h_{Lo}} \right]^2}$ $P = 0.00253 \text{Re}_{Lo}^{1.17} \text{Bo}^{0.6} (\phi_{MS} - 1)^{-0.65}$ $\phi_{MS} = \left[1 + 2 \left(\frac{1}{f_1} - 1 \right) x \text{Co}^{-1} \right] (1-x)^{1/3} + \frac{x^3}{f_2}$ For laminar flow: $f_1 = \frac{\rho_g \mu_l}{\rho_l \mu_g} \quad f_2 = \frac{\mu_g \text{Cp}_l}{\mu_l \text{Cp}_g} \left(\frac{k_l}{k_g} \right)^{1.5}$ For turbulent flow: $f_1 = \frac{\rho_g}{\rho_l} \left(\frac{\mu_l}{\mu_g} \right)^{0.25} \quad f_2 = \frac{k_g}{k_l}, \quad h_{nb} = h_{\text{Cooper}}$	47.62	51.40

6. Conclusions

Experimental findings on flow boiling heat transfer of R 134a in a vertical minichannel were reported in this study. Followings are the main findings,

- Heat transfer coefficient was strongly controlled by applied heat flux and no significant impact of varying mass flux and vapor quality was there.
- Increase in system pressure did increase the heat transfer performance.
- Most coherent and accurate predictions for local heat transfer coefficients were observed with Gungor and Winterton correlation [10].

7. Nomenclature

A_c	Cross sectional area [m ²]
Co	Confinement No [-]
C_p	Specific heat capacity [J/kg.K]
d_h	Inner diameter [m]
G	Mass Flux [kg/m ² s]
I	Current [A]
k	Thermal conductivity [w/m ² K]
L_h	heated length [m]
m'	Mass flow rate [kg/sec]
MBE	Mean Bias Error [%]
Q	Applied electric power [W]
q''	Heat Flux [W/m ²]
t_{sat}	Saturation temperature [°C]
V	Voltage [V]
We_D	Webber No [-]
x	Vapor quality [-]
z	Axial position [m]

Greek letters

μ	viscosity [Pa-s]
ρ	Density [kg/m ³]
σ	Surface Tension [N/m]

Subscript

g	gas phase
l	liquid phase

8 References

- [1] S. Kandlikar, Heat transfer and fluid flow in minichannels and microchannels, Elsevier, 2006.
- [2] C. M. Callizo, "Flow boiling heat transfer in single vertical channels of small diameters," KTH, Stockholm, 2010.
- [3] W. Owhaib, "Experimental heat transfer, pressure drop and flow visualization of R-134a in vertical mini/micro tubes," Doctoral Thesis in Energy Technology KTH, Stockholm, 2007.
- [4] C. B. Tibirica and G. Ribatski, "Flow boiling heat transfer of R134a and R245fa in a 2.3 mm tube," International Journal of Heat and Mass transfer, pp. 2459-2468, 2010.
- [5] C. L. Ong and J. R. Thome , "Macro-to-microchannel transition in two-phase flow: Part 2 – Flow boiling heat transfer and critical heat flux," Experimental thermal and fluid science, vol. 35, pp. 873-886, 2011.
- [6] T. N. Tran, M. W. Wambsganss and D. M. France, "Small circular and rectangular channel boiling with two refrigerants," International Journal of Multiphase flow, pp. 485-498, 1996.
- [7] G. Lazarek and S. H. Black, "Evaporative heat transfer, pressure drop and critical heat flux in a small vertical tube with R-113," International Journal of Heat and Mass transfer, pp. 945-960, 1982.
- [8] M. H. Maqbool, B. Palm and R. Khodabandeh, "Boiling heat transfer of ammonia in vertical smooth mini channels: Experimental results and predictions," International Journal of thermal sciences, pp. 1-9, 2011.
- [9] R. Ali, B. Palm and M. H. Maqbool, "Flow Boiling Heat Transfer Characteristics of a Minichannel Up to Dryout Condition," in ASME 2009 Second International Conference on Micro/Nanoscale Heat and Mass Transfer, Shanghai, 2009.

- [10] K. E. Gungor and R. Winterton, "A general correlation for flow boiling in tubes and annuli," *International Journal of Heat and Mass transfer*, pp. 351-358, 1986.
- [11] P. A. Kew and K. Cornwell, "Correlations for the prediction of boiling heat transfer in small diameter channels," *Applied Thermal Engineering*, pp. 705-715, 1997.
- [12] S. S. Bertsch, E. A. Groll and S. V. Garimella, "A composite heat transfer correlation for saturated flow boiling in small channels," *International Journal of Heat and Mass transfer*, pp. 2110-2118, 2009.
- [13] M. Cooper, "Saturated nucleate pool boiling, a simple correlation," in *Proceedings of the 1st UK National Heat Transfer conference*.
- [14] Z. Liu and R. H. S. Winterton, "A general correlation for saturated and subcooled flow boiling in tubes and annuli, based on a nucleate pool boiling equation," *International Journal of Heat and Mass transfer*, pp. 2759-2766, 1991.
- [15] D. Mikielwicz, "A new method for determination of flow boiling heat transfer coefficient in conventional diameter channels and minichannels," *Heat Transfer Engineering*, pp. 276-287, 2010.